Theor Chem Account (2009) 122:67–76
DOI 10.1007/s00214-008-0485-9

REGULAR ARTICLE

Theoretical study on the reaction mechanism of $CH_2SH + NO_2$

Yi-Zhen Tang · Ya-Ru Pan · Bing He · Jing-Yu Sun · Xiu-Juan Jia · Hao Sun · Rong-Shun Wang

Received: 27 July 2008 / Accepted: 22 September 2008 / Published online: 22 October 2008

Abstract The mechanisms of CH_2SH with NO_2 reaction were investigated on the singlet and triplet potential energy surfaces (PES) at the BMC-CCSD//B3LYP/6-311 + G(d,p) level. The result shows that the title reaction is more favourable on the singlet PES thermodynamically, and it is less competitive on the triplet PES. On the singlet PES, the initial addition of CH_2SH with NO_2 leads to $HSCH_2NO_2$ (IM2) without any transition state, followed by a concerted step involving C–N fission and shift of H atom from S to O giving out CH_2S + trans-HONO, which is the major products of the title reaction. With higher barrier height, the minor products are $CH_2S + HNO_2$, formed by a similar concerted step from the initial adduct $HSCH_2ONO$ (IM1). The direct abstraction route of H atom in SH group abstracted by O atom might be of some importance. It starts from the addition of the reactants to form a weak interaction molecular complex (MC3), subsequently, surmounts a low barrier height leading to another complex (MC2), which gives out CH_2S + trans-HONO finally. Other direct hydrogen abstraction channels could be negligible with higher barrier heights and less stable products.

Y.-Z. Tang · Y.-R. Pan · J.-Y. Sun · X.-J. Jia · H. Sun · R.-S. Wang (✉)
Institute of Functional Material Chemistry,
Faculty of Chemistry, Northeast Normal University,
Renmin Road 5268, Changchun, 130024 Jilin,
People's Republic of China
e-mail: wangrs@nenu.edu.cn

Y.-Z. Tang
e-mail: tangyz171@nenu.edu.cn

B. He
The Department of Chemistry, Sichuan College of Education,
610041 Chengdu, People's Republic of China

Keywords $CH_2SH \cdot NO_2 \cdot$ Transition state · Mechanism

1 Introduction

The combustion of the organic sulphur compounds and coals rich of sulphur can produce methylthiyl radical, CH_3S and its isomer CH_2SH, which are important intermediate [1–3] and toxic atmospheric contamination. It is firmly believed to be one of the key intermediates of OH-initiated oxidation of DMS, especially in area where the amount of NO_3 and IO are low enough not to compete with the OH oxidation. The researches focus on two aspects of CH_3S and CH_2SH: (1) the characters of special species, such as spectrum and thermochemistry; (2) the kinetics and mechanisms of reactions involving CH_2SH and CH_3S.

The reactions of CH_3S with some species, such as O_2, O_3, NO_2, and NO have been investigating widely [4–9]. However, little attention has been paid to the reactions of CH_2SH. In 1992, Anastasi and Broomfield [10] reported the rate constant of 3.5×10^{-11} cm^3 mol^{-1} s^{-1} at 1 atm and 298 K for the reaction of $CH_2SH + NO_2$ with the pulse radiolysis/kinetic absorption technique employed. Three possible reaction routes were presumed:

$$CH_2SH + NO_2 \rightarrow HSCH_2NO_2 \quad (1)$$

$$CH_2SH + NO_2 \rightarrow [HSCH_2ONO] \rightarrow HSCH_2O + NO \quad (2)$$

$$CH_2SH + NO_2 \rightarrow CH_2SH + HNO_2 \quad (3)$$

They proposed that the title reaction proceeds via addition. Although the mechanisms of $CH_2OH + NO_2$ reaction, similar to the title reaction, have been studied recently [11], no result was reported about the mechanisms for the title reaction. In this paper, we studied the title

reaction with high-level quantum methods for the first time, and hope it is beneficial to further experimental and theoretical study.

2 Computational methods

Density Functional Theoretical and ab initio calculations were carried out using the Gaussian 03 programs [12]. The geometries of reactants (R), transition states (TS), intermediates (IM), molecular complexes (MC), and products (P) were optimized employing the B3LYP method with the 6-311 + G(d,p) basis set. B3LYP method was proved to be an economic and accurate computational model for predicting electronic structure, and have been employing widely. Compared with other levels of theory, the B3LYP method was found to be sufficiently accurate for predicting reliable geometries of the stationary points, at the same time, it is not expensive computationally for scanning the potential energy surface (PES). To determine the nature of all species and the zero-point energy (ZPE) corrections, harmonic vibrational frequencies were calculated at the same level. The number of imaginary frequency (0 or 1) confirms whether a local minimum or a transition state. Subsequently, the intrinsic reaction coordinate (IRC) paths were calculated at the same level to verify the transition states connect to the right reactants and products. In order to obtain more reliable energy on the PES, the singlet-point-energy calculations were performed at the higher levels of G3MP2 [13, 14] and BMC-CCSD [15, 16].

BMC-CCSD scheme was detailed elsewhere, and only a brief description is given here. Singlet-point-energy evaluations were performed at the CCSD/6-31B(d) and MP2/MG3 levels of theory, respectively. Finally, the energy expression for BMC-CCSD is given in:

$$\begin{aligned} &E(\text{BMC-CCSD}) = E(\text{HF/6-31B(d)}) \\ &+ c_{\text{H}}\Delta(\text{HF/MG3}|\text{6-31B(d)}) + c_1\Delta(\text{MP2}|\text{HF/6-31B(d)}) \\ &+ c_2\Delta(\text{MP2}|\text{HF/MG3}|\text{6-31B(d)}) \\ &+ c_3\Delta(\text{MP4(DQ)}|\text{MP2/6-31B(d)}) \\ &+ c_4\Delta(\text{CCSD}|\text{MP4(DQ)/6-31B(d)}) + E_{\text{SO}} \end{aligned}$$

where $\Delta E(\text{L2}|\text{L1/B}) = E(\text{L2/B}) - E(\text{L1/B})$, $\Delta E(\text{L/B2}|\text{B1}) = E(\text{L/B2}) - E(\text{L/B1})$ and $\Delta E(\text{L2}|\text{L1/B2}|\text{B1}) = E(\text{L2/B2}) + E(\text{L1/B1}) - E(\text{L1/B2}) - E(\text{L2/B1})$.

And c_{H}, c_1, c_2, c_3, and c_4 take values of 1.06047423, 1.09791, 1.33574, 0.90363, and 1.55622, respectively.

3 Results and discussion

The geometries of all reactants, products, possible intermediates, molecular complexes and transition states involved in the reaction of CH_2SH with NO_2 are shown in Figs. 1 and 2. The singlet and triplet PES of the title reaction at the BMC-CCSD level are depicted in Figs. 3 and 4. Tables 1 and 2 exhibit the ZPE corrections, relative energies including ZPE corrections (ΔE, relative to the reactants of $CH_2SH + NO_2$), reaction enthalpies (ΔH), reaction Gibbs free energies (ΔG) at the B3LYP/6-311 + G(d,p), BMC-CCSD and G3MP2 levels. From Table 1 we can see that the energy obtained at the level of G3MP2 is in reasonable accordance with that from BMC-CCSD calculations. For the system of NO_2 and CH_2SH, it is radical–radical reaction, so it can occur on both of the singlet and triplet surfaces. The triplet species are signed 3 as superscript, and the energy obtained at the BMC-CCSD level is used in the discussion unless otherwise stated. In order to give a clear reaction progression, Fig. 5 describes the reaction channels on both the singlet and triplet PES.

3.1 The mechanisms on the singlet PES

3.1.1 Formation of initial adducts

The spin density is 0.455e for N atom, and 0.272e for each O atom in NO_2, therefore, both N and O atom could add to the C centre in CH_2SH radical. As shown in Fig. 1, IM1 and IM2 are the initial adducts by the addition of O and N atom to CH_2SH radical, respectively. In IM1, the newly formed C–O bond is about 1.43 Å, and the N–O bond is stretched by about 0.25 Å compared with its equilibrium in reactants. In IM2, the formed C–N bond is as long as 1.53 Å, while the N–O bond is only 0.03 Å longer than that in NO_2 molecule. Both the two addition processes are barrierless, confirmed by the scan calculation of the C–O and C–N bond, and exothermic by about 52 kcal/mol. It is noted that IM1 has two isomers depending on the dihedral angle ONOC, i.e., 180° and 0°, donated as IM1 and IM1′ in Fig. 1. The interconversion of IM1 and IM1′ takes place by the terminal N–O bond rotating around the adjacent N–O bond. In the corresponding transition state TS1, the dihedral angle ONOC is about 80°. With the barrier height (TS1) of 11.5 kcal/mol and the overall $\Delta G^{\neq}$ of −19.3 kcal/mol. the process is easy to occur. Energetically, IM1′ is almost equal to IM1, and the reaction enthalpy of the step is only 0.8 kcal/mol.

The result shows that IM1 and IM2 also could interconverse via a three-numbered-ring transition state, TS2, in which both the N–C and C–O bond is around 2.3 Å. The barrier height is rather high, about 59.9 kcal/mol for both direction of the conversion reaction IM1 → IM2, TS2 is even 8 kcal/mol above reactants on the PES, and the overall $\Delta G^{\neq}$ is 19.3 kcal/mol. It implies that the isomerization of IM1 and IM2 is difficult to proceed at room temperature or atmospheric condition.

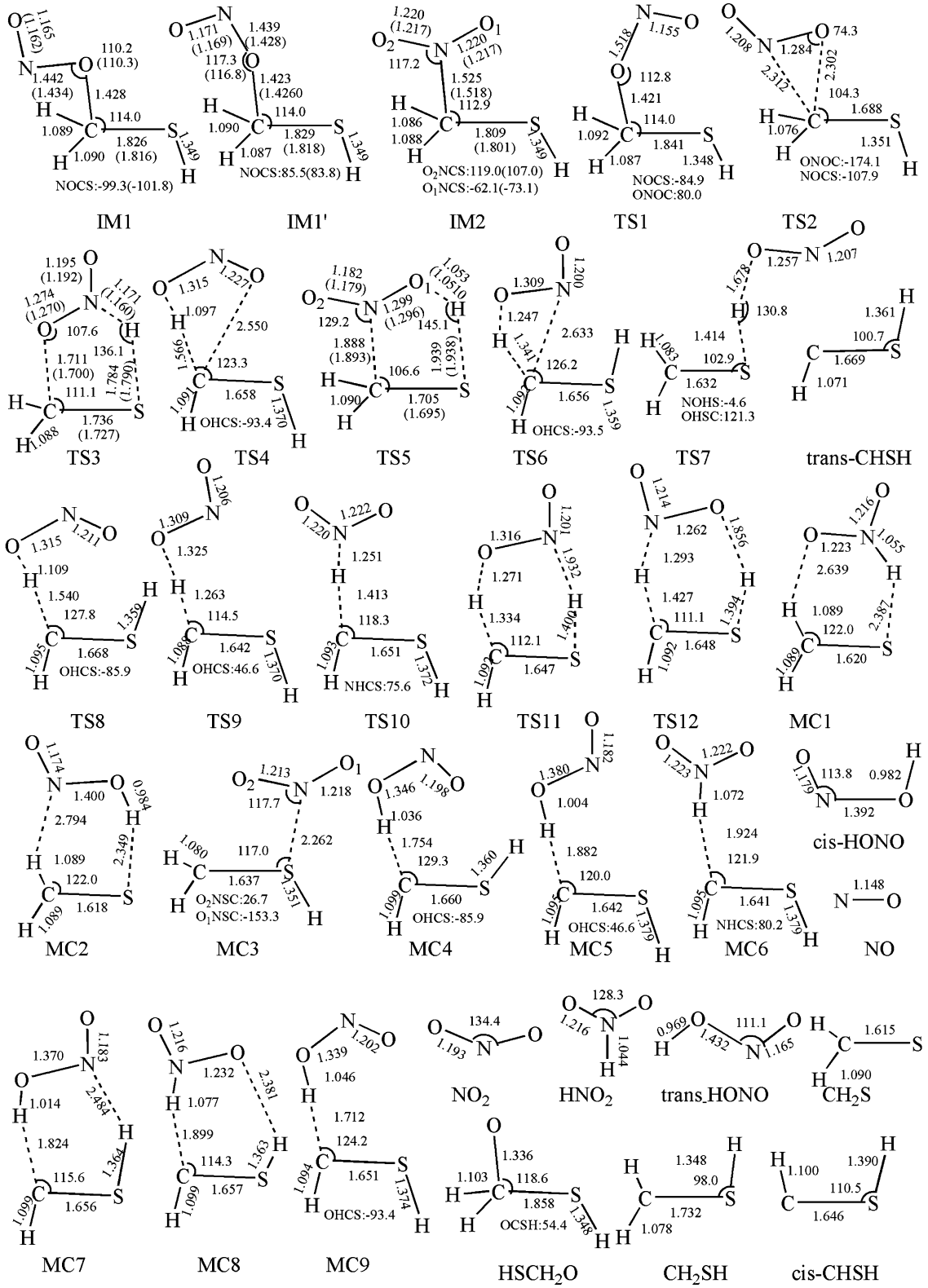

Fig. 1 The optimized geometries of all species for the $CH_2SH + NO_2$ reaction on the singlet PES at the B3LYP/6-311 + G(d, p) level. Bond lengths are in angstroms and angles in degree. In IM1, IM1′, IM2, TS3 and TS5, the values in parentheses are obtained at B3LYP/6-311 + G(3df, 3pd) level

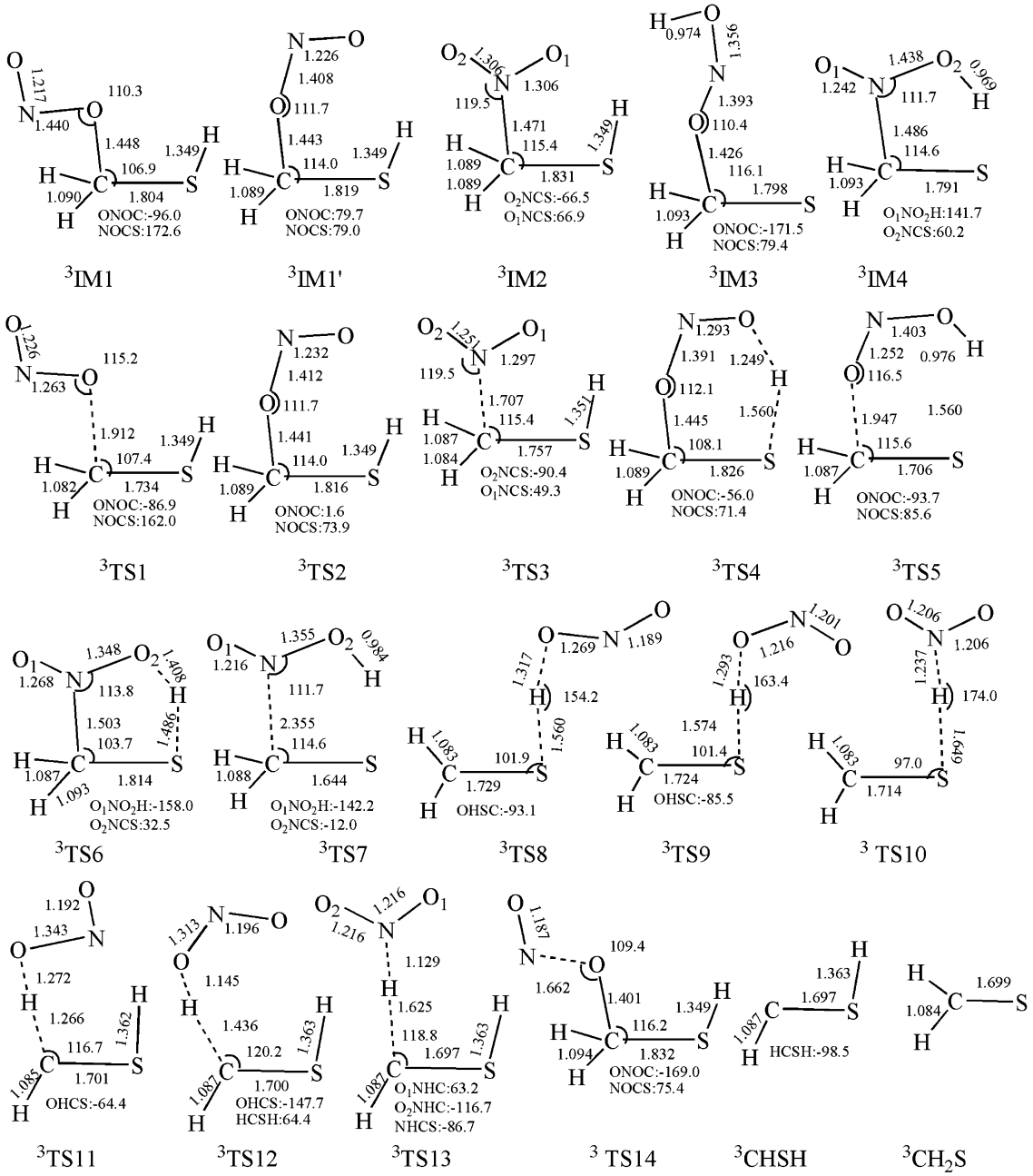

Fig. 2 The optimized geometries of all species for the $CH_2SH + NO_2$ reaction on the triplet PES at the B3LYP/6-311 + G(d,p) level. Bond lengths are in angstroms and angles in degree

With abundant energy available, it is feasible for further fragmentation or isomerization reaction. It will be discussed in the following part.

3.1.2 The mechanisms on the singlet PES

The formation of the initial adduct releases lots of energy, therefore, several channels could be opened.

The first possible channel from IM1 and IM1′ is the N–O bond fission leading to $HSCH_2O + NO$, about −10.3 kcal/mol below reactants. In spite of many attempts, no transition state was found for this process.

From IM1, the C–O bond dissociates and the H atom in SH group migrates to N atom simultaneously to give out $CH_2S + HNO_2$ via TS3, a five-numbered-ring transition state. In TS3, the broken C–O and S–H bond is about 1.71 and 1.78 Å, and the formed N–H is 1.17 Å, which is only 0.13 Å longer than its equilibrium value in product HNO_2. The barrier height is 35.9 kcal/mol, and this channel is exothermic by about 27.2 kcal/mol. The overall $\Delta G^{\neq}$ of

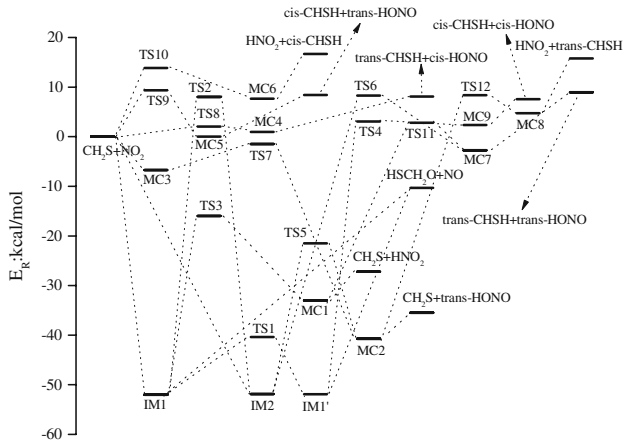

Fig. 3 The profile of singlet PES for the $CH_2SH + NO_2$ reaction at the BMC-CCSD//B3LYP/6-311 + G(d,p) level

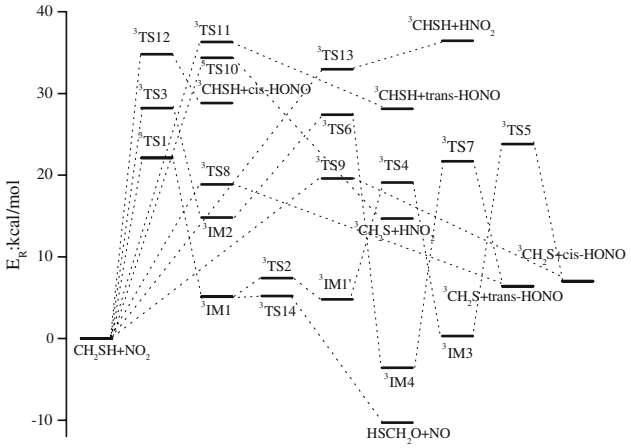

Fig. 4 The profile of triplet PES for the $CH_2SH + NO_2$ reaction at the BMC-CCSD//B3LYP/6-311 + G(d,p) level

TS3 is 1.8 kcal/mol, and the overall ΔG for this channel is −21.2 kcal/mol. The IRC calculation indicates that a hydrogen bond molecular complex (MC1) is involved in the forward direction. The long distance of H···O and S···H bond is around 2.64 and 2.39 Å, respectively. The stabilization energy of MC1 is about 33 kcal/mol. MC1 will give out to final products $CH_2S + HNO_2$, which also could be formed via other channels.

From IM1′, a similar concerted step is also possible to give out another products cis-HONO and cis-CHSH via a four-centre transition state TS4. The step involves the scission of C–O bond and the shift of H atom from C atom to the terminal O atom. In TS4, the broken C–O bond is around 2.55 Å, while the C–H bond is stretched by about 0.48 Å compared with that in IM1′. Energetically, TS4 is 3 kcal/mol higher than that of reactants with the barrier height of 55 kcal/mol, and the overall $\Delta G^{\neq}$ is 19.2 kcal/mol. The IRC calculation suggests that TS4 goes forward to MC9, in which the distance of C···H bond is about 1.71 Å. MC9 is about 2.3 kcal/mol on the PES, only 0.7 kcal/mol lower than TS4, and the formation of cis-HONO + cis-CHSH is endothermic by 8.9 kcal/mol with the overall $\Delta G^{\neq}$ is 19 kcal/mol. Obviously, with the tight barrier and so large $\Delta G^{\neq}$ of TS4 and the unstable products of cis-HONO + cis-CHSH, this channel is difficult to occur at room temperature condition. With a tight four-numbered-ring transition state, it is easy to understand that the energy of TS4 is higher than that of TS3.

Similar to the channel from IM1, the formation of CH_2S + trans-HONO takes place via a concerted step from IM2. In the corresponding transition state, TS5, a five-numbered-ring structure, the ruptured C–N and S–H bond is stretched by about 24 and 43% compared with that in IM2, while the formed H–O bond is 1.05 Å, only 0.08 Å longer than its equilibrium value in products trans-HONO. TS5 is about 21.5 kcal/mol below the initial reactants on the singlet PES. A weak interaction molecular complex MC2 was found to connect TS5 and CH_2S + trans-HONO. In MC2, a six-numbered-ring structure, the H···N and S···H bond is 2.79 and 2.35 Å, respectively. MC2 is 40.7 kcal/mol lower than reactants and the overall ΔG is −24.1 kcal/mol, and this channel is highly exothermic by 35.5 kcal/mol. With the barrier height of 30.4 kcal/mol and the overall $\Delta G^{\neq}$(TS5) of −3.6 kcal/mol, thermodynamically, this channel is more feasible to occur than the two channels stated above. Another possible scenario from IM2 is that one of the H atoms in CH_2 group shifts to one O atom and the C–N bond breaks simultaneously via TS6, in which the C–N and C–H bond is elongated to be 2.63 and 1.34 Å, respectively, while the H–O bond is 1.25 Å. The barrier height is about 60.2 kcal/mol, and TS6 is 8.3 kcal/mol on the PES. MC7, trans-CHSH···trans-HONO, is connected by TS6 in the forward direction and about −2.7 kcal/mol lower than reactants. MC7 gives out to trans-CHSH + trans-HONO finally, with this channel endothermic by 7.5 kcal/mol. As shown in Table 1, the overall ΔG of TS6, MC7, and trans-CHSH + trans-HONO is 21.3, 15, and 16.6 kcal/mol, respectively. Evidently, with so tight barrier of TS6 and unstable products, the formation of trans-CHSH + trans-HONO is less competitive with that of CH_2S + trans-HONO.

In order to check the influence of basis set, the 6-311 + G(3df,3pd) basis set is employed with the same method to reoptimize the geometries of some intermediates and transition states involved. The 6-311 + G(3df,3pd) basis set, which is useful for describing the interactions between electrons in electron correlation methods, puts 3d functions and 1f function on heavy atoms, and 3p functions and 1d function on hydrogen, as well as diffuse functions on both. The results are summarized in Fig. 1, from which it could be seen, the geometrical parameters are in reasonable agreement with those at the 6-311 + G(d,p) level.

Table 1 The ZPE corrections and relative energies ΔE (including ZPE corrections), reaction Enthalpies ΔH, and Gibbs Free Energies ΔG at B3LYP, G3MP2 and BMC-CCSD levels for the reaction of $CH_2SH + NO_2$ on the singlet PES (in kcal/mol)

Species	ZPE	ΔH	ΔG	ΔE_{B3LYP}	ΔE_{G3MP2}	ΔE_{BMC}
R: $CH_2SH + NO_2$	25.0	0.0	0.0	0.0	0.0	0.0
$CH_2S + HNO_2$	29.2	−23.9	−21.2	−23.1	−24.8	−27.2
CH_2S +cis-HONO	28.1	−29.9	−27.5	−29.21	−33.2	−34.9
CH_2S +trans-HONO	28.1	−30.9	−28.5	−30.3	−33.8	−35.5
HNO_2 + cis-CHSH	26.8	23.3	25.3	24.0	20.4	16.7
HNO_2 + trans-CHSH	27.3	21.8	23.9	22.6	19.4	15.8
cis-CHSH + cis-HONO	25.6	17.2	19.0	17.8	12.0	8.9
cis-CHSH + trans-HONO	25.7	16.3	18.0	16.8	11.4	8.4
trans-CHSH + cis-HONO	26.1	15.8	17.6	16.4	11.04	8.1
trans-CHSH + trans-HONO	26.2	14.8	16.6	15.4	10.43	7.5
$HSCH_2O$ + NO	25.3	−12.7	−11.1	−12.4	−12.1	−10.3
IM1	30.0	−45.5	−32.3	−43.3	−48.6	−51.9
IM1′	29.9	−44.7	−31.2	−44.2	−48.7	−52.0
IM2	31.1	−45.5	−32.1	−43.9	−47.7	−51.9
TS1	29.1	−33.1	−19.3	−31.5	−37.1	−40.4
TS2	28.0	6.7	19.3	7.9	9.4	8.0
TS3	29.0	−12.9	1.8	−10.9	−12.4	−16.0
TS4	26.1	6.1	19.2	7.4	6.2	3.0
TS5	30.0	−18.0	−3.6	−16.1	−18.0	−21.5
TS6	25.6	8.9	21.3	10.0	11.2	8.3
TS7	27.8	−2.8	10.7	−1.3	−0.8	−1.5
TS8	26.1	4.6	17.5	5.9	5.1	2.0
TS9	25.1	11.7	24.0	12.8	12.3	9.3
TS10	25.2	13.4	25.1	14.4	16.5	13.9
TS11	25.4	4.7	17.9	6.1	5.8	2.8
TS12	25.6	9.9	22.9	11.2	11.5	8.4
MC1	30.3	−28.3	−17.8	−27.7	−30.57	−33.0
MC2	29.5	−34.6	−24.1	−34.1	−38.7	−40.7
MC3	28.9	−4.9	7.3	−3.9	−5.6	−6.7
MC4	27.3	6.2	16.9	6.9	4.0	1.0
MC5	27.4	6.5	16.7	7.0	3.1	0.0
MC6	28.1	12.6	22.5	13.2	11.2	7.7
MC7	28.0	3.3	15.0	4.2	0.3	−2.7
MC8	28.6	9.6	21.3	10.5	8.2	4.7
MC9	27.0	7.4	19.0	8.2	5.5	2.3

Most changes in bond length and angles are less than 0.1 Å and 3°, except for the dihedral angle O_1NCS and O_2NCS, in which the difference is about 12°. Therefore, it could be concluded that addition of multiple polarization functions has no significant effect on the title reaction.

The direct hydrogen abstraction mechanism was also determined for the title reaction on the singlet PES. As shown in Figs. 1 and 3, four direct abstraction channels were located to form different products. The H atom in SH group could be abstracted by one O atom in NO_2 to from CH_2S + trans-HONO via TS7. In TS7, the S–H bond is elongated by only 0.07 Å compared with that in CH_2SH, and the new formed H–O bond is stretched by about 73% compared with its equilibrium value in trans-HONO. Therefore, TS7 is a reactant-like transition state, and the process occurs via an early transition state. The IRC calculation shows that each molecular complex was involved in the backward and forward directions, donated as MC3 and MC2 in Fig. 1, respectively. In MC3, the long distance of weak interaction between N and S atom is about 2.26 Å, and the C–S bond is about 0.1 Å shorter than that in reactants. MC3 is about 6.7 kcal/mol lower than reactants, and TS7 is about −1.5 kcal/mol on the singlet PES. TS7 and CH_2S + trans-HONO are connected by MC2, which is detailed stated above. With the barrier height of only 5.2 kcal/mol, obviously, this channel is favourable to

Table 2 The ZPE corrections and relative energies ΔE (including ZPE corrections) at B3LYP, G3MP2 and BMC-CCSD levels for the reaction of $CH_2SH + NO_2$ on the triplet PES (in kcal/mol)

Species	ZPE	ΔE_{B3LYP}	ΔE_{G3MP2}	ΔE_{BMC}
R:$CH_2SH + NO_2$	25.0	0.0	0.0	0.0
$^3CH_2S + HNO_2$	27.3	13.7	14.2	14.7
$^3CH_2S$ + trans-HONO	26.2	7.6	5.8	6.4
$^3CH_2S$ + cis-HONO	26.2	6.5	5.1	7.0
$^3CHSH + HNO_2$	26.2	38.4	36.4	36.4
^{3}CHSH + trans-HONO	25.1	32.2	28.0	28.1
^{3}CHSH + cis-HONO	25.1	31.2	27.4	28.8
^{3}IM1	29.0	4.2	4.7	4.8
^{3}IM1′	28.7	4.3	5.1	5.1
^{3}IM2	29.3	11.5	14.8	14.8
^{3}IM3	30.6	0.95	−0.3	0.3
^{3}IM4	30.8	−4.1	−3.7	−3.6
^{3}TS1	27.5	14.8	20.2	22.2
^{3}TS2	28.8	7.7	7.5	7.4
^{3}TS3	27.7	23.2	27.8	28.2
^{3}TS4	27.0	16.9	19.5	19.1
^{3}TS5	28.1	18.4	22.9	23.8
^{3}TS6	27.5	21.0	31.2	27.4
^{3}TS7	28.4	19.4	22.8	21.7
^{3}TS8	24.2	13.7	19.1	18.9
^{3}TS9	24.5	14.1	20.8	19.4
^{3}TS10	24.7	22.4	33.0	34.4
^{3}TS11	22.4	33.0	36.6	33.7
^{3}TS12	23.0	28.5	30.4	32.7
^{3}TS13	24.7	31.6	33.0	33.0
^{3}TS14	27.7	4.0	5.5	5.2

proceed dynamically. The overall $\Delta G^{\neq}$(TS7) of 10.7 cal/mol indicates that it might be less predominant to occur than the addition mechanism thermodynamically.

As for the direct hydrogen abstraction by O or N atom to produce CH_2S + cis-HONO or HNO_2, no transition state was located although many attempts made.

The H atom in CH_2 group abstracted by O or N atom leads to CHSH + HONO or HNO_2. The first possible channel is that O atom abstracts H atom to form trans-CHSH + cis-HONO via TS8. It could be seen from Fig. 1, the stretched C–H bond is about 1.54 Å, while the formed H–O bond is 1.11 Å. MC4, in which the distance of C atom and H atom is 1.75 Å, is confirmed to connect TS8 at the forward direction. TS8 and MC4 stand at 2 and 1 kcal/mol on the PES, respectively, and this channel is endothermic by 8.1 kcal/mol. The overall ΔG of TS8 and MC4 is 17.5 and 16.9 kcal/mol, respectively. The second route involves O atom abstracting H atom to form trans-HONO + cis-CHSH via TS9, in which the C–H and H–O bond is 1.26 and 1.33 Å. TS9 goes forward to MC5, in which the C···H

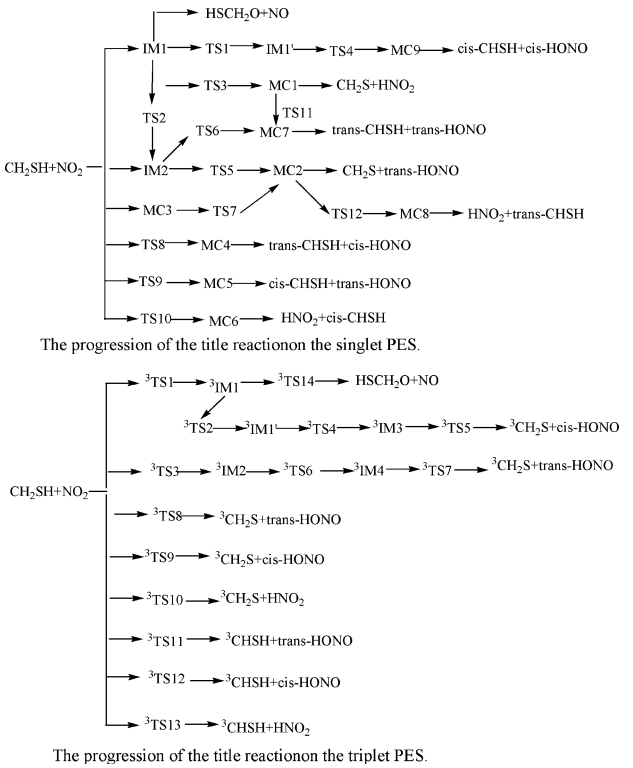

Fig. 5 Brief description of the progression on singlet and triplet PES for the $CH_2SH + NO_2$ reaction

is about 1.88 Å. The barrier height is 9.3 kcal/mol, while MC5 is equal to reactants. While the overall ΔG of TS9 and MC5 is 24 and 16.7 kcal/mol. The final products of trans-HONO + cis-CHSH is 8.4 kcal/mol higher than the reactants on the PES. The last possible channel involved is that N atom abstracts one H atom in CH_2 to form cis-CHSH + HNO_2 via TS10. The broken C–H bond and the formed H–N bond in TS10 are about 1.41 and 1.25 Å, respectively. MC6 connects TS10 and products, and the C···H is as long as 1.92 Å in MC6. TS10 and MC6 are 13.9 and 7.7 kcal/mol, respectively, on the PES. The overall ΔG of TS10 and MC6 is 25.1 and 22.5 kcal/mol. This process is endothermic by 16.7 kcal/mol and the ΔG is 25.3 kcal/mol. We attempt to locate any transition state in the direct hydrogen abstraction mechanism to form cis-CHSH + cis-HONO, trans-HONO + trans-CHSH and trans-CHSH + HNO_2, unfortunately, all calculations were failed due to the problem of convergence. However, these products could be yielded by the isomerization between products.

Obviously, with higher barrier heights and less stable products compared with that in isomerization reaction from adducts, the three channels are of no importance at atmospheric or room temperature condition.

As shown in Fig. 3, trans-HONO + trans-CHSH also could be formed from $CH_2S + HNO_2$ via a six-centred transition state TS11. In TS11, the stretched C–H and H–N

bond is 1.33 and 1.93 Å, respectively, while the formed H–O and H–S bond is as long as 1.27 and 1.40 Å. The IRC calculation indicates that TS11 is connected by MC1 and MC7, which were stated in above part. TS11 is 2.8 kcal/mol on the PES, which is about 35.8 kcal/mol higher than MC1. Another six-numbered-ring structure transition state TS12 was located to connect CH_2S + trans-HONO and HNO_2 + trans-CHSH. TS12 goes backward to MC2, and forward to MC8, in which the long distance of C···H and O···H bond is about 1.90 and 2.38 Å, respectively. MC8, TS12 and HNO_2 + trans-CHSH are about 4.7, 8.4 and 15.8 kcal/mol higher than reactants on the PES.

In summary, the fragmentation of the initial adducts (IM1 and IM2) gives out to CH_2S + HNO_2 and trans-HONO. Kinetically and thermodynamically, with lower barrier height and more stable products, the most feasible channel is that the shift of H atom in SH group to O atom and the scission of C–N bond from IM2 to form CH_2S + trans-HONO. The secondary channel is the shift of H atom in SH group to N atom and the scission of C–O bond from IM1 to form CH_2S + HNO_2. With less stable products, the barrierless N–O bond fission from IM1 and IM1′ produces $HSCH_2O$ +NO is of less importance thermodynamically. The most important hydrogen abstract channel dynamically is R → MC3 → TS7 → MC2 → CH_2S + trans-HONO. The stabilization energy of MC3 is less than that of the initial adduct and higher reaction Gibbs free energy, however, it might compete with the fragmentations channel at high temperature condition.

The initial adducts formation releases lots of heat to impulse further reaction steps, and more heat it releases, more feasible the channel is. Therefore, the addition mechanism is more favourable than the hydrogen abstraction mechanism on the singlet PES. From the aspect of pressure, the initial step starts from two molecules to form intermediates (IM1 or IM2). With the incensement of pressure, the reaction is more favourable to form adducts. It is easy to understand that it is more favourable to form the final products. As for hydrogen abstraction channel, it is almost pressure independence.

3.2 The mechanisms on the triplet PES

3.2.1 The formation of initial adducts

Similar to the addition of initial reactants on the singlet PES, both N and O atoms could associate to the C centre in CH_2SH on the triplet PES. However, the entrance reactions take place to form the initial adducts via tight barriers. As seen in Fig. 2, the O atom attacks C atom to generate ^{3}IM1, in which the dihedral angles ONOC and NOCS are about −96° and 173°, respectively. The formation of ^{3}IM2 is the result of N atom adding to C centre, and the dihedral angles O_1NCS and O_2NCS are about −67° and 67°. Different to that on the singlet PES, the addition processes occur via tight barriers, namely, ^{3}TS1 and ^{3}TS3 shown in Fig. 3, respectively. In ^{3}TS1, the newly formed C–O bond is about 1.91 Å, which is about 0.46 Å longer than that in product ^{3}IM1. While in ^{3}TS3, the newly formed C–N bond is 1.71 Å, only 0.24 Å longer than the value of 1.47 Å in ^{3}IM3. The barrier heights of ^{3}TS1 and ^{3}TS3 are 22.2 and 28.2 kcal/mol, and the addition processes are endothermic by 4.8 and 14.8 kcal/mol, respectively. ^{3}IM1 could converse into ^{3}IM1′ via ^{3}TS2, in which the dihedral angles ONOC and NOCS are about 1.6° and 74°, respectively. While in ^{3}IM1′, ONOC and NOCS are about 80° and 79°, respectively. With barrier height of 2.6 kcal/mol, the conversion between ^{3}IM1 and ^{3}IM1′ is easy to proceed. Energetically, ^{3}IM1′ is only 0.3 kcal/mol lower than ^{3}IM1. Although many attempts made, transition states involving the steps of R → ^{3}IM1′ and ^{3}IM1 → ^{3}IM2 were not located.

With the high barrier heights and unstable initial adducts, the triplet PES is less feasible than that on the singlet PES. However, several channels are considered in our calculations.

3.2.2 The mechanisms on the triplet PES

The direct N–O bond dissociation of ^{3}IM1 produces $HSCH_2O$ + NO via ^{3}TS14, in which the broken N–O bond is 1.66 Å. ^{3}TS14 is only 0.1 kcal/mol higher than ^{3}IM1 on the triplet PES, and this process is exothermic by about 10.3 kcal/mol. Obviously, once ^{3}IM1 is formed, it is quickly and easily to produce $HSCH_2O$ + NO.

The second possible channel takes place by the rearrangement of ^{3}IM1′. Once the intermediate was formed, the H atom in SH group will migrate to the terminal O atom leading to ^{3}IM3 via a six-numbered-ring structure ^{3}TS4. The broken S–H bond in ^{3}TS4 is stretched by about 0.21 Å compared with its equilibrium value in ^{3}IM1′, and the formed H–O bond was about 1.25 Å. The barrier height is about 14 kcal/mol, and the energy of ^{3}IM3 is almost equal to reactants. Subsequently, the C–O bond dissociates to give out $^3CH_2S$ + cis-HONO via ^{3}TS5, in which the C–O bond is as long as 1.95 Å. The two moieties connected by the broken C–O bond in ^{3}TS5 stand as spectator. ^{3}TS5 is about 23.8 kcal/mol above the initial reactants, and this channel is endothermic by about 7 kcal/mol.

From ^{3}IM2, the formation of $^3CH_2S$ + trans-HONO occurs by the rearrangement reaction similar to the channel stated above. The H-shift from S tom to O atom leads to ^{3}IM4 via a five-numbered-ring structure transition state ^{3}TS6. The S–H and O–H bond is about 1.49 and 1.41 Å in ^{3}TS6, respectively. In ^{3}IM4, the N-O_2 bond is stretched by 0.13 Å compared with that in ^{3}IM2, while N-O_1 bond is

shorten by only 0.06 Å. ^{3}TS6 and ^{3}IM4 stand at 27.4 and −3.6 kcal/mol on the triplet PES. The scission of C–N bond in ^{3}IM4 gives to the final products $^3CH_2S$ + trans-HONO via ^{3}TS7. The barrier height is about 25.3 kcal/mol, and the products are 6.4 kcal/mol higher than reactants.

The direct hydrogen abstraction pathways were also located on the triplet PES. The H atom in SH group is abstracted by O and N atom to form $^3CH_2S$ + trans-HONO, cis-HONO and HNO_2 via ^{3}TS3, 8TS9 and ^{3}TS10, respectively. In the corresponding transition states, the broken S–H bond and the formed H–O (H–N) bond is about 1.56, 1.57, 1.65 and 1.32, 1.29, 1.24 Å, respectively. The barrier heights are 18.9, 19.6 and 34.4 kcal/mol, and the channels are endothermic by 6.4, 7, and 14.7 kcal/mol.

Moreover, the H atom in CH_2 group also could be abstracted by O and N atoms. The products of ^{3}CHSH + trans-HONO, cis-HONO and HNO_2 are formed via ^{3}TS11, ^{3}TS12 and ^{3}TS13, respectively, in which the C–H and H–O (H–N) bond is about 1.27, 1.44, 1.63 and 1.27, 1.15, 1.13 Å. The barrier heights are rather high, about 33.7, 32.7 and 33 kcal/mol, and the three abstraction channels are endothermic by 28.1, 28.8 and 36.4 kcal/mol, respectively.

In brief, the barrier heights on the triplet PES are much higher than that on the singlet PES, therefore, the triplet PES might be negligible at room temperature and atmospheric condition. However, the most feasible channel on the triplet PES is direct hydrogen abstraction to form $^3CH_2S$ + trans-HONO. With the barrier height of only 0.7 kcal/mol higher than that of the most feasible channel, $^3CH_2S$ + cis-HONO would compete with the above channel.

3.3 The comparisons with $CH_2OH + NO_2$ and $CH_3S + NO_2$ reactions

It is very important to compare the PES feature of the $CH_2SH + NO_2$ reaction with that of analogous $CH_2OH + NO_2$ reaction. Theoretically, only Zhang et al. [11] reported detailed mechanisms of CH_2OH with NO_2 reaction at the G3//B3LYP/6-311G(d,p) level. The results show that the reaction proceeds mostly on the singlet PES, and the entrance reaction is barrierless. The major products for $CH_2OH + NO_2$ reaction are CH_2O + trans-HONO, which was formed by a concerted step involving the C–N bond fission and H atom shift in the initial adduct $HOCH_2NO_2$. The minor products including HOCHO + HNO, CH_2O + HNO_2 and CH_2O + cis-HONO are less competitive with the dominant ones. The comparisons between the two reactions indicate that the most feasible channel and major products, besides minor products, are similar on the theoretical level. However, many unfavourable channels revealed in the reaction of $CH_2OH + NO_2$ were not considered for the title reaction. The direct hydrogen abstraction mechanism was not mentioned in CH_2OH + NO_2 reaction, while our calculation suggests it might give some contributions at high temperature or combustion condition.

On the other hand, the reaction of $CH_3S + NO_2$, is also important in combustion chemistry. Recently, we built up the PES of CH_3S reaction with NO_2 at the QCISD(T)/6-311 ++G(d,p)//B3LYP/6-311 ++G(d,p) level [9]. The initial barrierless addition leads to CH_3SONO, followed by a barrierless N–O bond scission to give out $CH_3SO + NO$, which is the major products. Similar to the title reaction, the $CH_3S + NO_2$ reaction is more predominant on the singlet PES; however, no transition state was located for direct hydrogen abstraction mechanism. It is worth noting that the CH_3SNO_2 could isomerise to $HSCH_2ONO$ via a rather tight barrier, therefore, it could be said that $CH_3S + NO_2$ and $CH_2SH + NO_2$ reactions take place on the same PES, expect for the direct hydrogen abstraction channels.

4 Conclusions

The mechanisms for CH_2SH with NO_2 reaction were investigated on the singlet and triplet PESs at the BMC-CCSD//B3LYP/6-311 + G(d,p) level. In addition, the singlet-point energy is calculated at the G3MP2//B3LYP/6-311 + G(d,p) level. The result shows that the title reaction is more favourable on the singlet PES energetically, and it is less competitive on the triplet PES. On the singlet PES, the initial addition of CH_2SH with NO_2 leads to $HSCH_2NO_2$ (IM2) without any transition state, followed by a concerted step involving C–N fission and the shift of H atom from S to O atom giving out CH_2S + trans-HONO, which is the major products for the title reaction. With higher barrier height, the minor products are $CH_2S + HNO_2$, formed by a similar concerted step from the initial adduct $HSCH_2ONO$ (IM1). It is worth noting that all stationary points involving in the two channels above are below the reactants. The direct abstraction route of H atom in SH group abstracted by O atom might be of some importance at high temperature or combustion condition. It starts from the addition of the reactants to form a weak interaction molecular complex (MC3), subsequently, surpasses a low barrier height leading to another complex (MC2), and gives out CH_2S + trans-HONO. Other direct hydrogen abstraction channels could be negligible with higher barrier heights and less stable products. It is in good accordance with Anastasi's presumption that the reaction proceeds via addition mechanism.

Acknowledgments This work was supported by the National Natural Science Foundation of China (No. 20773021) and the Science Foundation for Young Teachers of Northeast Normal University (No. 20070315). We are greatly thankful for the referees' helpful comments.

References

1. Atkinson R, JN Pitts Jr, Aschrmann SM (1984) J Phys Chem 88:1584
2. Yin F, Grosjean D, Seinfeld JH (1990) J Atmos Chem 11:309
3. Wine PH, Kreutter NM, Gump CA, Ravishankara AR (1981) J Phys Chem 85:2660
4. Tyndall GS, Ravishankara AR (1989) J Phys Chem 93:2426
5. Martinez E, Albaladejo J (2000) Atmos Environ 34:5295
6. Wang SK, Zhang QZ, Zhou JH, Gu YS (2004) Acta Chimica Sinica 62:550
7. Martinez E, Albaladejo J (1999) Chem Phys Lett 308:37
8. Chang PF, Wang TT, Wang NS (2000) J Phys Chem A 104:5525
9. Tang YZ, Sun H, Pan YR, Wang RS (2007) Int J Quantum Chem 107:1495
10. Anastasi C, Broomfield M (1992) J Phys Chem 96:696
11. Zhang JX, Li ZS, Liu JY, Sun CC (2006) J Phys Chem A 110:2690
12. Frisch MJ, Trucks GW, Schlegel HB, Scuseria GE, Robb MA, Cheeseman JR, Zakrzewski VG, Montgomery JA, Stratmann RE, Burant JC, Dapprich S, Millam JM, Daniels AD, Kudin KN, Strain MC, Farkas O, Tomasi J, Barone V, Cossi M, Ayala PY, Cui Q, Morokuma K, Malick DK, Rabuck AD, Raghavachari K, Foresman JB, Gomperts R, Martin RL, Fox DJ, Keith T, Al-Laham MA, Peng CY, Nanayakkara A, Gonzalez C, Challacombe M, Gill PMW, Johnson BG, Chen W, Wong MW, Andres JL, Head-Gordon M, Replogle ES, Pople JA (1998) Gaussian 03; Gaussian, Pittsburgh PA
13. Curtiss LA, Raghavachari K, Redfern PC, Pople JA (1998) J Chem Phys 109:7764
14. Baboul AG, Curtiss LA, Raghavachari K (1999) J Chem Phys 110:7650
15. Fast PL, Corchado JC, Truhlar DG (1999) J Phys Chem A 103:5129
16. Lynch BJ, Zhao Y, Truhlar DG (1999) J Phys Chem A 109:1643